The Astrophysical Journal Letters, 846:L15 (5pp), 2017 September 10 https://doi.org/10.3847/2041-8213/aa8506

The Formation of Rapidly Rotating Black Holes in High-mass X-Ray Binaries

Aldo Batta[1], Enrico Ramirez-Ruiz[1], and Chris Fryer[2,3]
[1] Department of Astronomy and Astrophysics, University of California, Santa Cruz, CA 95064, USA
[2] Department of Physics, The University of Arizona, Tucson, AZ 85721, USA
[3] CCS Division, Los Alamos National Laboratory, Los Alamos, NM 87545, USA
Received 2017 June 1; revised 2017 August 1; accepted 2017 August 2; published 2017 September 1

Abstract

High-mass X-ray binaries (HMXRBs), such as Cygnus X-1, host some of the most rapidly spinning black holes (BHs) known to date, reaching spin parameters $a \gtrsim 0.84$. However, there are several effects that can severely limit the maximum BH spin parameter that could be obtained from direct collapse, such as tidal synchronization, magnetic core-envelope coupling, and mass loss. Here, we propose an alternative scenario where the BH is produced by a *failed* supernova (SN) explosion that is unable to unbind the stellar progenitor. A large amount of fallback material ensues, whose interaction with the secondary naturally increases its overall angular momentum content, and therefore the spin of the BH when accreted. Through SPH hydrodynamic simulations, we studied the unsuccessful explosion of an 8 $M_\odot$ pre-SN star in a close binary with a 12 $M_\odot$ companion with an orbital period of $\approx$1.2 days, finding that it is possible to obtain a BH with a high spin parameter $a \gtrsim 0.8$ even when the expected spin parameter from direct collapse is $a \lesssim 0.3$. This scenario also naturally explains the atmospheric metal pollution observed in HMXRB stellar companions.

Key words: binaries: close – supernovae: general

1. Introduction

To date, we know of the existence of a handful of high-mass X-ray binaries (HMXRBs) harboring stellar mass black holes (BHs). The BHs in these systems are characterized by having a large spin parameter $a > 0.8$ (Liu et al. 2008; Gou et al. 2009, 2014), which are difficult to reconcile with the classical formation scenario of HMXRBs where the BH is formed from the direct collapse (or *failed* supernova, SN) of a massive star in a close binary. An HMXRB can result in this scenario provided that there is low mass loss from the failed SN and the BH experiences either a small natal kick that induces no significant orbital change or a strong kick in a restricted direction that results in a final close orbit. For stellar binaries forming short-period HMXRBs ($\lesssim$1 day), tidal synchronization is expected to be effective (van den Heuvel & Yoon 2007). This tidal locking constrains the total angular momentum content available to form the BH. Even in the absence of tidal locking, the maximum BH spin parameter can be restricted by the interior of the star being spun down either by magnetic coupling (Spruit 2002) or mass loss.

Assuming that synchronization induces rigid body rotation, Lee et al. (2002) calculated the BH spin expected from direct collapse. They found that for typical orbital periods (of a few days), the maximum spin parameter is $a \lesssim 0.4$.[4] What is more, the final spin of the BH depends on the mass distribution of the pre-SN star, which differs significantly from a polytropic one. In fact, more realistic pre-SN mass distributions yield more compact cores, which produce even smaller spin parameters, thus severely hampering the formation of rapidly rotating BHs in typical HMXRBs.

Alternatively, as has been observed in red giants (Beck et al. 2012), it is possible that the core of the pre-SN star decouples from the slower rotating, tidally locked outer layers. Such rapidly rotating cores, commonly found in some pre-SN progenitor models (Heger et al. 2000; Woosley & Heger 2006), could produce a rapidly rotating BH from the collapse of the Fe core. However, when tidal forces are effective in bringing a significant fraction of the stellar progenitor to synchronous rotation, a BH formed from a rapidly rotating core will be naturally slowed down as it accretes the slowly rotating outer layers. This implies that the only way to get a rapidly rotating BH from a star with a slowly rotating envelope is from the interaction with the companion or from external mass accretion.

The accretion rate in HMXRBs can, however, only be a small fraction of the companion's mass-loss rate, typically $\lesssim 10^{-5}\,M_\odot\ \mathrm{yr}^{-1}$ (Crowther 2007). This in turn places an upper limit on the amount of mass that the BH could have accreted, given the short lifetime of the companion ($\approx 10^5$ years for WR stars). While high BH spins in low-mass XRBs can be acquired via mass transfer (Fragos & McClintock 2015), as shown by King & Kolb (1999) and Podsiadlowski et al. (2003), this is not the case for HMXRBs. In such systems, it has been widely believed that the properties of BHs are primarily natal (Liu et al. 2008; Valsecchi et al. 2010; Axelsson et al. 2011).

Here, we propose an alternative scenario in which the spin of the BH comes from accretion of fallback material ejected during a failed SN explosion. To this end, we ran a series of 3D smoothed particle hydrodynamics (SPH) simulations of the ejection and fallback of the low-velocity, tidally locked stellar envelope in a close binary with a massive companion and an orbital period that is typical of HMXRBs. In what follows, we study the properties of pre-SN stars and the low-energy SN explosions that can result in large BH spins in HMXRBs as well as atmospheric metal pollution in the surviving stellar companions.

2. BH Formation and Fallback from Failed SNe in Binaries

In the classical formation scenario, the HMXRB progenitor begins as a detached binary with a mass ratio $q = M_\mathrm{p}/M_\mathrm{c} > 1$. As the primary of mass M_p evolves, a mass transfer episode is

[4] For comparison, the spin of a BH expected from the collapse of a maximally rotating polytropic star is $a \approx 0.75$ (Shapiro & Shibata 2002).

triggered. With $q > 1$, the mass transfer is likely to become unstable once the donor develops an extended convective envelope or evolves to become a red supergiant. This will shrink the binary orbit so efficiently that a common envelope phase will be triggered (Tauris & van den Heuvel 2006). As a result, the primary can end up as a He star accompanied by a more massive companion with an orbital period of a few days. Tidal synchronization of its components might not be attained before the primary reaches the end of its life (van den Heuvel & Yoon 2007); however, magnetic coupling between the core and the stellar envelope (Spruit 2002), or mass loss preceding BH formation, could strongly reduce the amount of angular momentum in the primary.

Once the primary exhausts its nuclear fuel and reaches the pre-SN stage, the collapse of the Fe core will lead to the formation of a proto-neutron star (PNS), which will inject energy into the infalling stellar layers through its copious neutrino emission. The shock produced by this energy injection will move outward decelerating the infalling layers and forcing them out. Shocked material with velocities smaller than the escape velocity will ultimately fall back onto the newly formed PNS. The subsequent formation of a BH will depend on the amount of fallback material, which, in turn, depends strongly on the energy injected and the structure of the star (Fryer et al. 2012; Ugliano et al. 2012; Pejcha & Thompson 2015). It is believed that the nature of failed SNe might be responsible for shaping the galactic black hole mass function (Özel et al. 2010; Kochanek 2015, 2014).

The outcome of the failed SNe scenario could range from the quiet disappearance of a star producing no observable transient, to the production of low-luminosity transients (Fryer et al. 2009; Moriya et al. 2010; Dexter & Kasen 2013; Lovegrove & Woosley 2013; Piro 2013). The amount and structure of fallback material will be mainly determined by the currently unknown properties of the explosion, which, in turn, depends on the debated structure of the stellar progenitor at the end of its life (Perna et al. 2014). Recent observational evidence suggests that these failed explosions may not be that uncommon (Kochanek et al. 2008; Reynolds et al. 2015; Adams et al. 2017) and that the assembly of BH binaries (GW150914 and GW151226) observed by the Laser Interferometer Gravitational-wave Observatory (LIGO) may necessitate a failed SN scenario (Abbott et al. 2016a, 2016b; Belczynski et al. 2016) in order to explain the large BH masses inferred.

A weak or failed SN explosion is expected to be produced during the collapse of a non-negligible fraction of massive stars (Nadezhin 1980; Lovegrove & Woosley 2013; Piro 2013). In such instances, energy injection fails to completely unbind the star such that a sizable fraction of its mass eventually falls back onto the newly formed BH. If this takes place within a close binary, a fraction of the stellar material can expand to a radius comparable to or larger than the binary's separation, thus engulfing the companion. The capture of such low-velocity SN ejecta by a close companion could explain the overabundances of α elements (O, Mg, Si, S) observed in the companion stars of X-ray binary systems (Israelian et al. 1999; Podsiadlowski et al. 2002; Willems et al. 2005; González Hernández et al. 2008, 2011; Suárez-Andrés et al. 2015). Eventually, the interaction with the companion can torque the fallback material around the newly formed BH, thus effectively changing its angular momentum content. It is to this issue that we now turn our attention.

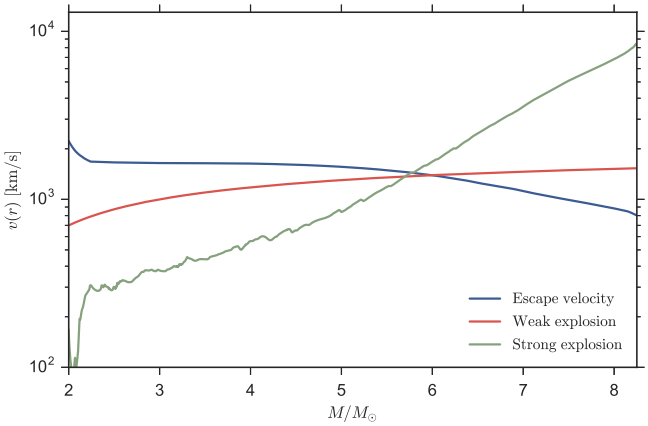

Figure 1. Radial velocity profiles (green and red lines) and escape velocity (blue line) as a function of the inner mass $M(r)$ contained within the radius r, for the two explosion scenarios explored here. The (relatively) strong (green line) and failed (red line) SN explosions have kinetic to binding energy ratios of $\sigma = E_{\rm kin}/E_{\rm bin} = 3.75$ and $\sigma = 0.77$, respectively. Both explosions have very similar fallback masses of $M_{\rm fb} \approx 6\,M_\odot$, which include the initial mass of the BH.

2.1. Setup for SPH simulations

To study whether or not the interaction of fallback material with the recently formed BH–star binary could translate into a sizable increase in the overall angular momentum of the material accreted onto the BH, we perform a series of 3D SPH simulations using a modified version of GADGET2 (Springel 2005). In particular, we study the expansion and fallback of a low-velocity, tidally locked stellar envelope in a close binary hosting a 12 $M_\odot$ companion in a 1.2 day orbit. The density, velocity, and internal energy profile of the envelope was derived from the SN explosion of an 8 $M_\odot$ helium core of a 25 $M_\odot$ KEPLER model from Woosley et al. (2002), with slightly varied parameters as described in C. Fryer et al. (2017, in preparation). The collapse is modeled using a 1D core-collapse code including a coupled equation of state covering a broad range of densities; a gray flux-limited, three-species neutrino diffusion scheme; a small nuclear network; and a spherically symmetric, post-Newtonian general relativistic (GR) routine (Herant et al. 1994; Fryer et al. 1999). After the collapse and bounce, we remove the core and use a parameterized energy injection routine mimicking the convection-enhanced SN engine to produce a range of explosion energies and remnant masses. Our study focuses on an explosion that produces reasonable remnant masses for our study. We considered the innermost 2 solar masses of the pre-SN star to be the newly formed BH with an initial spin $a = 0$, which we treat as a sink particle.

Three different scenarios are explored. The first considers the direct collapse of the envelope without any energy injection. The second uses the successful though weak SN model discussed above, in which the explosion has a kinetic to binding energy ratio $\sigma = E_{\rm kin}/E_{\rm bin} = 3.75$ (where $E_{\rm bin} = 1.3 \times 10^{50}$ erg) resulting in the high-velocity ejection of about one-third of the envelope. In the third scenario, we adopted a shallower velocity profile, representing a very weak (failed) SN explosion with a kinetic to binding energy ratio $\sigma = 0.77$. Figure 1 shows the two different velocity profiles used in our simulations as a function of the inner mass coordinate M. The blue line represents the escape velocity of the envelope, and the green and red lines represent the velocity profiles for the successful and failed SN explosions, respectively. Both

explosions have a very similar fallback mass of $M_{\rm fb} \approx 6\,M_\odot$ but very different velocity profiles, which leads to a very different interaction between the fallback material and the binary. These different interactions result in varying accretion histories, which ultimately determine the BH's final mass and spin.

The 1D SN explosion models are mapped into a 3D spherically symmetric distribution of SPH particles. This distribution is obtained by constructing spherical shells with $N_{\rm shell}$ particles evenly distributed across the shell's surface using HEALPix (Górski et al. 2005). The number of particles in each shell is determined by the local density $\rho(r)$, the total number of SPH particles $N_{\rm sph}$, and the particle masses $m_i = M_f/N_{\rm sph}$. After running a series of convergence tests for the accretion rate onto the BH with $N_{\rm sph}$ ranging from 5×10^5 to 1×10^7, we settled for a resolution of $N_{\rm sph} \simeq 2 \times 10^6$.

2.2. Accretion onto the BH

Since the resolution of the simulation gradually decreases as particles are accreted and material escapes, we had to implement an accretion prescription. An accretion radius of $r_{\rm acc} < 0.01\,R_\odot$ from the BH is defined, within which particles are accreted if certain conditions are met. Particles within $r_{\rm acc}$ falling toward the BH with less specific angular momentum than the one needed to orbit at the innermost circular stable orbit ($j < j_{\rm isco}$) are considered to be accreted. These particles transfer their entire mass and angular momentum to the BH. Particles within $r_{\rm acc}$, falling toward the BH and with specific angular momentum $j_{\rm crit} \leqslant j < 10 j_{\rm crit}$, are also considered to be accreted. These particles are assumed to be accreted via an accretion disk in a viscous timescale $t_\nu \approx \alpha^{-1}(H/R)^{-2} 1/\Omega_{\rm k}$, where $\Omega_{\rm k} = (GM_{\rm bh}/r_{\rm disk}^3)^{1/2}$, $H/R \approx 0.1$, and $\alpha \approx 0.1$. These particles transfer $j = j_{\rm isco}$ to the BH (with the rest assumed to be effectively transported outward) and have a fraction of their rest mass radiated away as in Bardeen (1970) and Thorne (1974).

3. Results

Figure 2 shows the evolution of the BH's spin parameter as a function of the accreted mass together with the corresponding accretion rates obtained for the three scenarios explored here. The accretion of subcritical material ($j < j_{\rm crit}$) transfers its angular momentum directly to the BH, while supercritical material ($j \gtrsim j_{\rm crit}$) is only accreted after a viscous timescale, transferring $j = j_{\rm crit}$ (Bardeen 1970; Thorne 1974). Thus, there is a limit to the maximum amount of specific angular momentum that can be transferred to the BH via a disk. In general, the BH accretes material with mainly subcritical angular momentum that only marginally increases a.

The evolution of the BH spin in our simulations is shown as solid lines in the top panel of Figure 2. The BH has an initial spin of $a \simeq 0$, which increases as mass and angular momentum are accreted. In order to consider the scenario where the BH forms from a rapidly rotating core, which is decoupled from the synchronized envelope, we also calculate the evolution of an initially maximally rotating BH ($a \simeq 0.99$) accreting material as in our simulations. The evolution of this maximally rotating BH is shown as dashed lines in the top panel of Figure 2. Each line is colored according to the three scenarios explored: blue for direct collapse, green for a strong SN explosion, and red for a weak SN explosion. As the spin of the BH and its mass

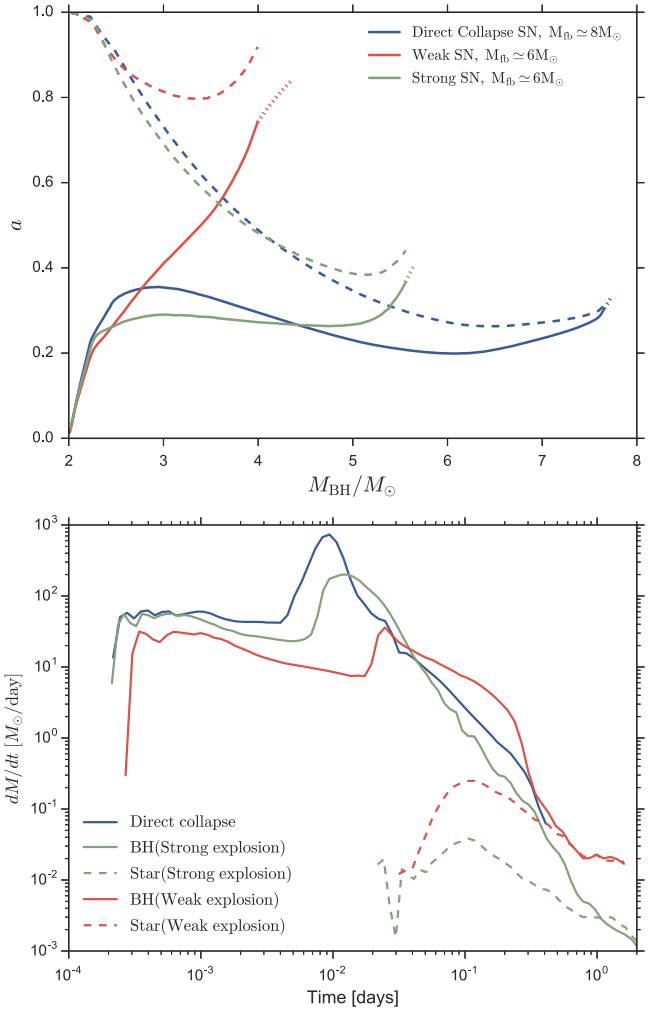

Figure 2. Spin parameter of the BH (top panel) as a function of the accreted mass for the three different scenarios explored here: a failed SN explosion (red line), a successful SN explosion (green line), and direct collapse (blue line). The solid lines correspond to our simulations, and the dashed lines indicate the evolution of the BH's spin assuming that a maximally rotating BH was formed from the core and accretes the same angular momentum and mass as in the simulations. The bottom panel shows the accretion rate evolution obtained for the BH and the companion.

determine the value of $r_{\rm isco}$ and the angular momentum accreted through a disk $j_{\rm isco}$, the evolution of the maximally rotating BH is only an approximation and overestimates to the total amount of angular momentum being accreted through a disk.

As can be seen in the lower panel from Figure 2, the accretion rates for the simulations with successful and failed SN explosions decrease to $\dot{M} \lesssim 10^{-2}\,M_\odot$ day^{-1} after $t \simeq 1$ day. With such low accretion rates, the simulation would require a prohibitively large CPU time to modestly increase the mass of the BH. We thus decided to stop the simulations at this point and obtain an estimate of the spin parameter assuming that all of the material bounded to the BH (and within its Roche lobe) will eventually be accreted through an accretion disk. The transition between the solid and dashed lines shown in the top panel of Figure 2 marks the end of the accretion rates derived from the simulation and the beginning of the analytical estimate (Bardeen 1970; Thorne 1974). This gives a robust upper limit to the spin parameter obtained from the accretion of such material. This estimate does not account for material outside the BH's Roche lobe, which, although still bounded to the

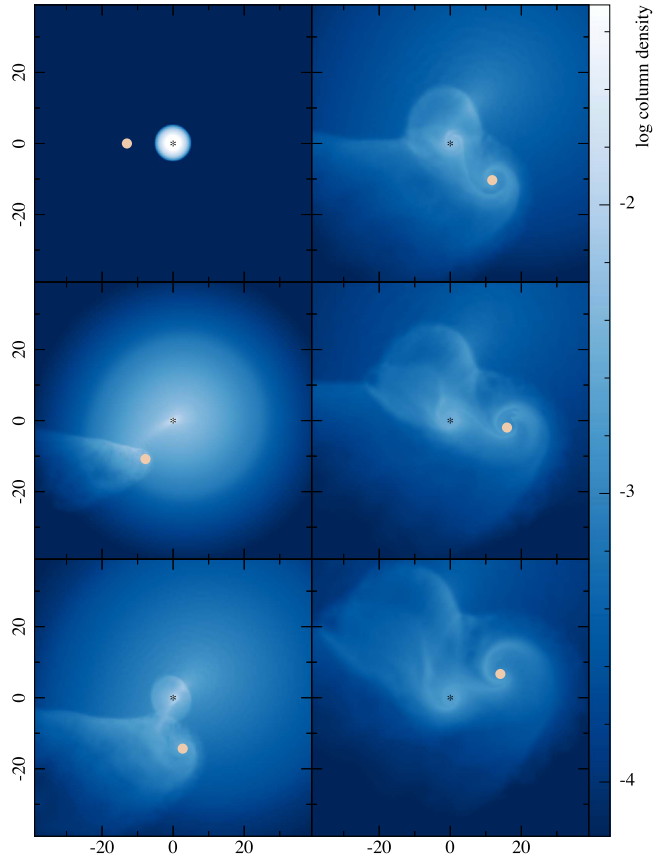

Figure 3. Column density of the failed SN ejecta integrated along the binary's rotation axis. The evolution of the companion (white dot) and the ejecta is being followed from the position of the recently formed BH (black dot). The distance scale is in $R_\odot$ units, and the box covers roughly 40 $R_\odot$ around the BH. The column density is scaled by $\Sigma_c = 4.1080 \times 10^{11}$ g cm^{-2}. The panels show the evolution up to $t = 1.1$ days, in time steps of $\Delta t = 0.185$ days, increasing from top to bottom and from left to right.

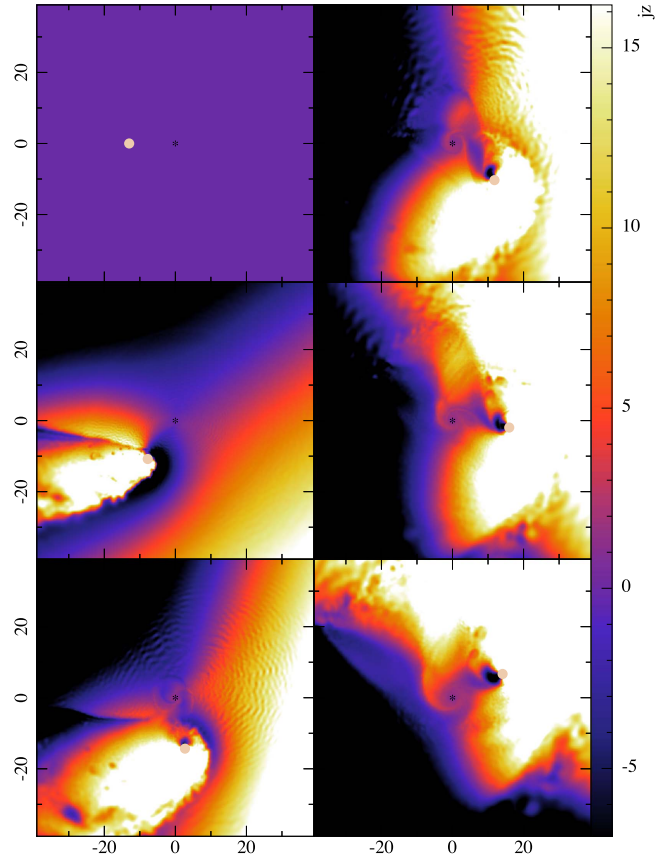

Figure 4. Evolution of the SN ejecta's specific angular momentum within the orbital plane as measured from the position of the BH. The color on the first panel corresponds to an initially small positive angular momentum $j_z \gtrsim 0$. Blue to black colors indicate negative values of j_z, while colors ranging from purple to red and white correspond to positive angular momentum larger than the initial value. The specific angular momentum is scaled by $j_c = 3.04 \times 10^{18}$ cm^2 s^{-1}. The panels show the same snapshots as in Figure 3.

system, it is likely to be accreted instead by the more massive companion.

As expected, the direct-collapse simulation gives rise to the smallest spin parameter ($a \approx 0.3$), which is without surprise similar to the one obtained by Lee et al. (2002). In the successful SN explosion calculation, a prompt collapse of the innermost $\approx$3.5 $M_\odot$ follows by the ejection of $\approx$2 $M_\odot$ of envelope material. In this case, only about $\approx$0.5 $M_\odot$ of material is able to be effectively torqued by the binary. In the failed SN explosion case, there is a substantial amount of material that interacts with the binary, and as a result, a circumbinary disk is produced. This results in a significant increase in the angular momentum content of the fallback material, which in turn increases the BH spin to $a \gtrsim 0.8$.

Figure 3 shows the evolution of the integrated column density (along the binary's rotation axis) in the failed SN explosion case. A large amount of material is observed to remain within $\approx$40 $R_\odot$ from the BH (the black dot is used as the rest frame in all panels) at the end of the simulation, which could be eventually accreted by the BH or the companion. The white dot indicates the position of the 12 $M_\odot$ companion star, which interacts gravitationally with the ejecta and the BH, and is allowed to accrete material using the same criteria that was used for the BH. It can be seen in the last panel of Figure 3 that each binary component has an accretion disk and eventually a circumbinary disk is formed around the binary. By the end of the fallback phase, the companion accretes $\approx$0.05 $M_\odot$ of low-velocity ejecta coming mostly from the original oxygen layer of the star. Since explosive nuclear burning occurs within this layer, the enriched infalling material will pollute the companion's atmosphere. Enrichment signatures have already been observed as overabundances of α elements (O, Mg, Si, S) in the companion stars of X-ray binary systems (Israelian et al. 1999; González Hernández et al. 2008, 2011; Suárez-Andrés et al. 2015) and might be explained by the capture of SN ejecta from a close companion.

Figure 4 shows the specific angular momentum j_z of the ejecta measured from the BH's position. Initially, all material is contained within $\approx$4 $R_\odot$ and has very small angular momentum. As the ejecta moves away from the recently formed BH, it is torqued by the companion. This causes material to lose or gain angular momentum according to its original position with respect to the companion. Such an effect can be seen in the second panel of Figure 4, where two distinct regions are clearly seen; the blue to black regions comprise material with specific angular momentum $j_z \leqslant 0$, torqued in the opposite direction of its original angular momentum, while the purple to red and white regions comprise material with $j_z > 0$ that gain angular momentum due to the interaction with the binary. From the third panel on, after about 0.55 days, it is evident that a centrifugally supported structure forms around the BH, whose subsequent accretion is able to spin up the BH.

Both the successful and failed SN explosions show the formation of an accretion disk around the binary before completing a full orbital period. However, the amount of accreted material is determined by the velocity profile of the explosion. In order to get a substantial fraction of the ejected mass to form a sizable accretion disk, the velocity profile of the bounded material must have velocities that are comparable to the escape velocity of the exploding progenitor. Material with $v_r \ll v_{\rm esc}$ will not get far from the BH and will promptly be accreted, thus drastically reducing the torque that could get from its interaction with the companion.

4. Conclusions

Through a series of 3D SPH simulations we have studied a scenario in which a rapidly rotating BH in an HMXRB can be produced following a failed SN explosion. We have studied three different scenarios for the SN explosion of the tidally locked stellar progenitor in a close binary system: direct collapse to a BH, a successful SN explosion with a large kinetic to binding energy ratio, and a failed SN explosion with a low kinetic to binding energy ratio. In the last case, the resulting velocity profile allows for a large fraction of the material to reach distances comparable to the separation of the binary.

Our simulations show that the angular momentum content of the SN material in a close binary system can be increased through its interaction with the binary companion. Material falling back from beyond the BH's Roche lobe can be significantly torqued by the companion, changing its trajectory and velocity toward the BH and ultimately increasing its angular momentum. As shown in the failed SN explosion case, in order to obtain a large gain in the angular momentum accreted by the BH, it is key for the ejecta to reach distances comparable to the binary's separation before falling back; otherwise, the angular momentum gain will be negligible. We thus conclude that the presence of rapidly rotating BHs in HMXRBs can potentially be explained by invoking a failed SN explosion mechanism, in which a large fraction of the stellar material is marginally bound.

ORCID iDs

Enrico Ramirez-Ruiz https://orcid.org/0000-0003-2558-3102
Chris Fryer https://orcid.org/0000-0003-2624-0056

References

Abbott, B. P., Abbott, R., Abbott, T. D., et al. 2016a, PhRvL, 116, 241103
Abbott, B. P., Abbott, R., Abbott, T. D., et al. 2016b, PhRvL, 116, 241103
Adams, S. M., Kochanek, C. S., Gerke, J. R., Stanek, K. Z., & Dai, X. 2017, MNRAS, 469, 1445
Axelsson, M., Church, R. P., Davies, M. B., Levan, A. J., & Ryde, F. 2011, MNRAS, 412, 2260
Bardeen, J. M. 1970, Natur, 226, 64
Beck, P. G., Montalban, J., Kallinger, T., et al. 2012, Natur, 481, 55
Belczynski, K., Holz, D. E., Bulik, T., & O'Shaughnessy, R. 2016, Natur, 534, 512
Crowther, P. A. 2007, ARA&A, 45, 177
Dexter, J., & Kasen, D. 2013, ApJ, 772, 30
Fragos, T., & McClintock, J. E. 2015, ApJ, 800, 17
Fryer, C. L., Belczynski, K., Wiktorowicz, G., et al. 2012, ApJ, 749, 91
Fryer, C. L., Benz, W., Herant, M., & Colgate, S. A. 1999, ApJ, 516, 892
Fryer, C. L., Brown, P. J., Bufano, F., et al. 2009, ApJ, 707, 193
González Hernández, J. I., Casares, J., Rebolo, R., et al. 2011, ApJ, 738, 95
González Hernández, J. I., Rebolo, R., Israelian, G., et al. 2008, ApJ, 679, 732
Górski, K. M., Hivon, E., Banday, A. J., et al. 2005, ApJ, 622, 759
Gou, L., McClintock, J. E., Liu, J., et al. 2009, ApJ, 701, 1076
Gou, L., McClintock, J. E., Remillard, R. A., et al. 2014, ApJ, 790, 29
Heger, A., Langer, N., & Woosley, S. E. 2000, ApJ, 528, 368
Herant, M., Benz, W., Hix, W. R., Fryer, C. L., & Colgate, S. A. 1994, ApJ, 435, 339
Israelian, G., Rebolo, R., Basri, G., Casares, J., & Martín, E. L. 1999, Natur, 401, 142
King, A. R., & Kolb, U. 1999, MNRAS, 305, 654
Kochanek, C. S. 2014, ApJ, 785, 28
Kochanek, C. S. 2015, MNRAS, 446, 1213
Kochanek, C. S., Beacom, J. F., Kistler, M. D., et al. 2008, ApJ, 684, 1336
Lee, C.-H., Brown, G. E., & Wijers, R. A. M. J. 2002, ApJ, 575, 996
Liu, J., McClintock, J. E., Narayan, R., Davis, S. W., & Orosz, J. A. 2008, ApJL, 679, L37
Lovegrove, E., & Woosley, S. E. 2013, ApJ, 769, 109
Moriya, T., Tominaga, N., Tanaka, M., et al. 2010, ApJ, 719, 1445
Nadezhin, D. K. 1980, Ap&SS, 69, 115
Özel, F., Psaltis, D., Narayan, R., & McClintock, J. E. 2010, ApJ, 725, 1918
Pejcha, O., & Thompson, T. A. 2015, ApJ, 801, 90
Perna, R., Duffell, P., Cantiello, M., & MacFadyen, A. I. 2014, ApJ, 781, 119
Piro, A. L. 2013, ApJL, 768, L14
Podsiadlowski, P., Nomoto, K., Maeda, K., et al. 2002, ApJ, 567, 491
Podsiadlowski, P., Rappaport, S., & Han, Z. 2003, MNRAS, 341, 385
Reynolds, T. M., Fraser, M., & Gilmore, G. 2015, MNRAS, 453, 2885
Shapiro, S. L., & Shibata, M. 2002, ApJ, 577, 904
Springel, V. 2005, MNRAS, 364, 1105
Spruit, H. C. 2002, A&A, 381, 923
Suárez-Andrés, L., González Hernández, J. I., Israelian, G., Casares, J., & Rebolo, R. 2015, MNRAS, 447, 2261
Tauris, T. M., & van den Heuvel, E. P. J. 2006, in Formation and Evolution of Compact Stellar X-ray Sources, ed. W. H. G. Lewin & M. van der Klis (Cambridge: Cambridge Univ. Press), 623
Thorne, K. S. 1974, ApJ, 191, 507
Ugliano, M., Janka, H.-T., Marek, A., & Arcones, A. 2012, ApJ, 757, 69
Valsecchi, F., Glebbeek, E., Farr, W. M., et al. 2010, Natur, 468, 77
van den Heuvel, E. P. J., & Yoon, S.-C. 2007, Ap&SS, 311, 177
Willems, B., Henninger, M., Levin, T., et al. 2005, ApJ, 625, 324
Woosley, S. E., & Heger, A. 2006, ApJ, 637, 914
Woosley, S. E., Heger, A., & Weaver, T. A. 2002, RvMP, 74, 1015